New Phytologist

Research

Tree tobacco (*Nicotiana glauca*) cuticular wax composition is essential for leaf retention during drought, facilitating a speedy recovery following rewatering

Boaz Negin[1,2], Shelly Hen-Avivi[1], Efrat Almekias-Siegl[1], Lior Shachar[1], Georg Jander[2] and Asaph Aharoni[1]

[1]Plant and Environmental Science Department, Weizmann Institute of Science, Rehovot 7610001, Israel; [2]Boyce Thompson Institute, 533 Tower Road, Ithaca, NY 14853, USA

Author for correspondence:
Asaph Aharoni
Email: asaph.aharoni@weizmann.ac.il

Received: *1 August 2022*
Accepted: *5 November 2022*

New Phytologist (2022)
doi: 10.1111/nph.18615

Key words: alkanes, drought, epicuticular wax, fatty alcohols, genome editing, *Nicotiana glauca*, plant fitness, tree tobacco.

Summary

- Despite decades of extensive study, the role of cuticular lipids in sustaining plant fitness is far from being understood. We utilized genome-edited tree tobacco (*Nicotiana glauca*) to investigate the significance of different classes of epicuticular wax in abiotic stress such as cuticular water loss, drought, and light response.
- We generated mutants displaying a range of wax compositions. Four wax mutants and one cutin mutant were extensively investigated for alterations in their response to abiotic factors.
- Although the mutations led to elevated cuticular water loss, the wax mutants did not display elevated transpiration or reduced growth under nonstressed conditions. However, under drought, plants lacking alkanes were unable to reduce their transpiration, leading to leaf death, impaired recovery, and stem cracking. By contrast, plants deficient in fatty alcohols exhibited elevated drought tolerance, which was part of a larger trend of plant phenotypes not clustering by a glossy/glaucous appearance in the parameters examined in this study.
- We conclude that although alkanes have little effect on whole *N. glauca* transpiration and biomass gain under normal, nonstressed conditions, they are essential during drought responses, since they enable plants to seal their cuticle upon stomatal closure, thereby reducing leaf death and facilitating a speedy recovery.

Introduction

Plants' aerial organs are exposed to a plethora of environmental conditions that require a protective barrier to shield the inner tissues from desiccation, high radiation in different wavelengths, and colonization or feeding by other organisms such as fungi, bacteria, and insects (Yeats & Rose, 2013). To cope with these abiotic and biotic stresses, plants have a complex surface layer, which may also contain specialized components that aid in responding to different factors. The cuticle may be imbedded with flavonoids (Ryan *et al.*, 2001, 2002; Mintz-Oron *et al.*, 2008; Adato *et al.*, 2009) and anthocyanins (Chalker-Scott, 1999) that reduce UVB damage to the mesophyll. Trichomes present on the surface may serve as a structural and chemical obstacle for plant herbivores (Hanley *et al.*, 2007) and also change leaf reflectance, thereby reducing photoinhibition and UVB-related damage (Steffens & Walters, 1991; Peiffer *et al.*, 2009; Bickford, 2016; Sonawane *et al.*, 2020).

The plant cuticle consists of three core elements localized beyond the epidermis cells. The cutin polymer is composed of an amorphous matrix primarily comprising C_{16} and C_{18} fatty acids and modified fatty acids such as ω-hydroxylated fatty acids, which often contain midchain hydroxyl or epoxy groups connected in esteric bonds (Yeats & Rose, 2013). The cutin polymer is also embedded with a substantial amount of carbohydrates adjacent to the cell wall, intracuticular wax in its more outer fraction, and epicuticular waxes, which are deposited beyond the cutin layer. It is clear that the cuticle plays a crucial role in preventing nonstomatal water loss, and certain wax components, such as long-chain alkanes, correlate with reduced cuticular permeability (Leide *et al.*, 2007, 2011). However, the extent to which epicuticular wax contributes to the transpirational barrier varies widely. Furthermore, in some cases, this contribution may be negligible compared to that of cutin and intracuticular waxes (Jetter & Riederer, 2016; Zeisler & Schreiber, 2016; Zeisler-Diehl *et al.*, 2018). This keeps open the question of epicuticular wax functions in cases where its contribution to the transpirational barrier is small. A related question is to what extent the different wax components contribute to the varied functions of epicuticular wax.

Decades of extensive research mainly using the model species *Arabidopsis thaliana* resulted in the elucidation of most biosynthetic pathways associated with the production of Arabidopsis surface wax components (Fig. 1; Lee & Suh, 2015). In Arabidopsis, fatty acids synthesized in plastids are transported to the endoplasmic reticulum (ER), where they are converted to acyl-CoA by

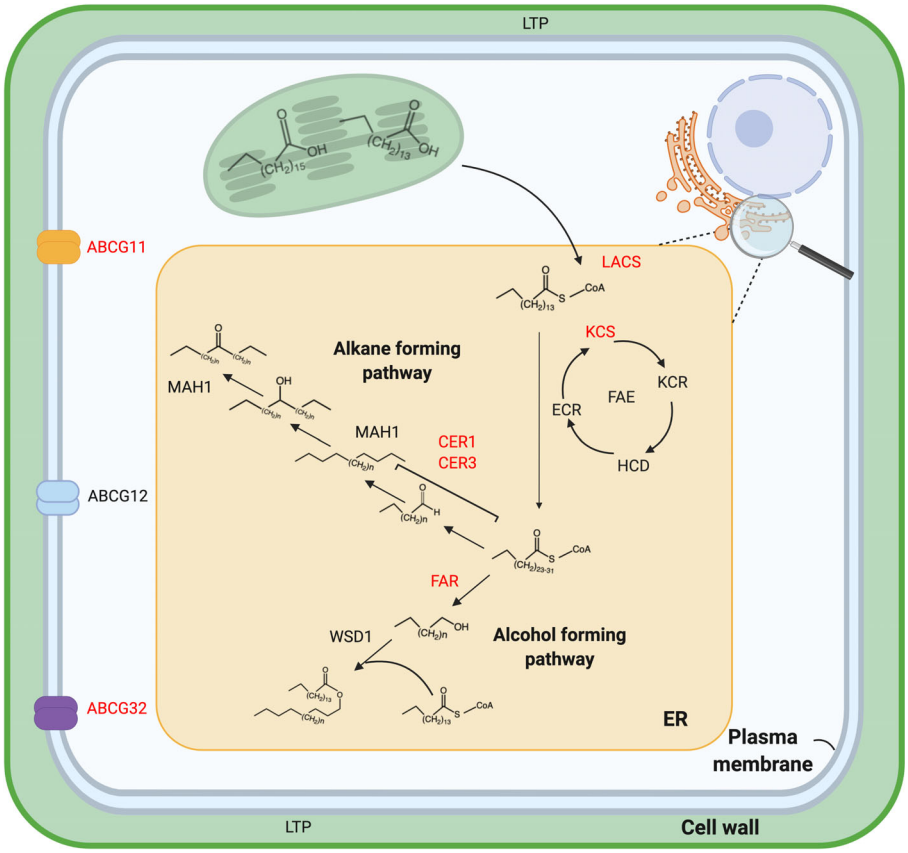

Fig. 1 Schematic model of epicuticular wax biosynthesis and transport pathways. Not all proteins involved in these pathways are presented, and genes corresponding to proteins marked in red were targeted for editing in *Nicotiana glauca* and exhibited a visual phenotype in this study. The scheme presents fatty acid elongation and division to the two main wax synthesis pathways: the alkane and fatty alcohol-forming pathways. Genes in which mutations were induced that are involved in wax synthesis but not in a specific pathway include *KCS6* and *LACS*. Those taking part in alkane synthesis are *CER1*, *CER3*, and *MAH1*, and fatty alcohol synthetic genes include *FAR* and *WSD1*.

LONG CHAIN ACYL SYNTHETASE (LACS) (Schnurr *et al.*, 2004; Lü *et al.*, 2009). The fatty acid elongase complex (FAE), which is composed of four proteins, then elongates these C_{16}–C_{18} precursors. These include (1) β-KETOACYL-COA SYNTHASE (KCS) (Millar & Kunst, 1997) having different variants responsible for elongation of certain acyl substrates (e.g. KCS6 targeted in this study is responsible for elongation from 24 to 34 carbons; Millar *et al.*, 1999), (2) β-KETOACYL-COA REDUCTASE (KCR; Beaudoin *et al.*, 2009), (3) 3-HYDROXYACYL-COA DEHYDRATASE (HCD; Bach *et al.*, 2008), and (4) *TRANS*-2,3-ENOYL-COA REDUCTASE (ECR; Zheng *et al.*, 2005). These enzymes elongate acyl-CoA through a cycle in which malonyl-CoA and the acyl are condensed, and at its end, the acyl is elongated by two carbons. The outcome of the elongation process is very long-chain fatty (VLCF) acyl-CoA of different lengths, used in several epicuticular wax biosynthesis pathways. They can be converted into very long-chain fatty acids (VLCFA) or enter two paths: the alkane- and alcohol-forming pathways. In the alkane-forming pathway, VLCF acyl-CoA is decarboxylated to create aldehydes and then alkanes. The exact enzymatic mechanisms taking place during the conversion of acyl-CoA to alkanes are not yet clear, though it is recognized that ECERIFERUM1 (CER1) and ECERIFERUM3 (CER3) take part in the initial stages of this process (Aarts *et al.*, 1995; Chen *et al.*, 2003; Bourdenx *et al.*, 2011). Following the synthesis of alkanes, these can be further modified to form secondary alcohols and ketones by the MID-CHAIN ALKANE HYDROXYLASE1 (MAH1), a cytochrome P450 catalyzing both reactions (Greer *et al.*, 2007). In the primary alcohol-forming pathway, VLCF acyl-CoA is converted to primary alcohols by adding a hydroxyl at the acyl's end. This step is catalyzed by the FATTY ACYL-COA REDUCTASE (FAR) enzyme (Rowland *et al.*, 2006). An additional stage in the alcohol-forming pathway is the conjugation of C_{16} or C_{18} fatty acids to the primary alcohols to create wax esters by the BIFUNCTIONAL WAX SYNTHASE/ACYL-COA: DIACYLGLYCEROL ACYLTRANSFERASE1 (WSD1; Li *et al.*, 2008). Although the presence of epicuticular wax is almost ubiquitous among plants, there is great diversity between species and even different organs of the same plant in the chemical structure and form of wax crystals they produce (Barthlott *et al.*, 1998; Lee & Suh, 2015).

Tree tobacco (*Nicotiana glauca*) is a perennial shrub, originating in South America, that has spread world-wide. The appearance of its stems and leaves is glaucous, an uncommon appearance in tobacco, which gave the species its Latin name. The glaucous appearance results from a high load of epicuticular wax coating the plant's aerial organs. This wax is composed almost solely of C_{31} alkanes, with lesser amounts of additional alkanes, fatty alcohols, and aldehydes (Mortimer *et al.*, 2012). Furthermore, *N. glauca* accumulates substantial amounts of wax in response to drought, while maintaining its original composition (Cameron *et al.*, 2006). These characteristics, as well as the availability of a genome sequence (Usadel *et al.*, 2018), efficient stable transformation, and the ease of dissecting the epidermis layer, make *N. glauca* an excellent model plant for studying the

yet unresolved role of epicuticular waxes in plant responses to the environment.

In this study, we employed CRISPR-Cas9 technology to mutate 16 cuticular lipid metabolism genes in *N. glauca*. Following initial molecular characterization, we carried out in-depth research on five selected knockout mutants that showed diverse patterns of wax composition. This mutant set was subjected to a range of experiments to help us better understand the contribution of epicuticular wax to plant fitness and attribute these effects to specific wax components. We found that, under optimal conditions, epicuticular wax has little effect on plant transpiration and biomass gain. By contrast, following drought, the alkane fraction is essential for leaf retention and therefore plant recovery, whereas deficiency in fatty alcohols did not affect plants negatively under our experimental conditions. Findings in this study highlight the specific role of plant epicuticular wax during episodes of drought and in the following recovery phase. They further explain how the diversity of wax components and structures contributes to plant fitness under abiotic stress conditions.

Materials and Methods

Plant material and growth conditions

Seeds of *N. glauca* Graham were initially collected from plants growing nearby the Weizmann Institute campus in Rehovot, Israel (31°54′45″N, 34°49′13″E). Plants used for transcriptome analysis were grown in soil containing tuff, peat, and slow-release fertilizer in the glasshouse in Rehovot, Israel, with no light supplementation (winter 2013). For cuticular wax and cutin extraction, scanning electron microscopy (SEM), stomatal analysis, cuticular water loss, and photosynthetic efficiency assays, plants were grown in a glasshouse in Rehovot in two batches during the winter–spring of 2019 and 2020 under similar conditions. Plants used for gum arabic wax extraction were grown in soil containing peat, fertilizer mix (Peter's Professional 11-5-11 Uni-mix, Everris North America Inc., North Charleston, SC, USA), lime (Microfine Dolomite, National, Findlay, OH, USA), vermiculite, and slow-release fertilizer (Osmocote Plus 15-9-12, Everris North America Inc., North Charleston, SC, USA) in a glasshouse in Ithaca, NY, USA, during the winter–spring of 2022. Supplemental light was added from high-pressure sodium lamps once ambient lighting dropped below 350 μmol m^{-2} s^{-1}. Plants used for light curves were grown in a growth room under a photosynthetic photon flux density of *c.* 150 μmol m^{-2} s^{-1}, at 22°C, and with a 16 h : 8 h, light : dark photoperiod. Drought experiments were performed using the Plantarray (PlantDitech, Yavne, Israel) screening platform located at the Israeli Center of Research Excellence (ICORE) for Plant Adaptation to the Changing Environment, at The Hebrew University of Jerusalem, Rehovot, Israel (31°54′15″N, 34°48′4″E), during July–September 2018, January–March 2019, and April–May 2020.

CRISPR vectors and mutation analysis

Construct assembly was performed using the 'golden braid' cloning system (Sarrion-Perdigones *et al.*, 2013). For details of vectors and mutation analysis, see Supporting Information Methods S1 and Fig. S1.

Transcriptomics and differential gene analysis

Transcriptome analysis was performed on several plant tissues under well-watered and drought conditions (induced by three events of drying and recovery as described in Cameron *et al.*, 2006). In this instance, well-watered plants were irrigated in excess using a drip system in the glasshouse, whereas drought-treated plants were not irrigated until wilting was observed, after which irrigation was resumed. RNA extraction, library preparation, and RNA-seq were performed as described in Hen-Avivi *et al.* (2016). Since the *N. glauca* genome was unpublished during analysis of the raw reads, we performed *de novo* transcriptome assembly based on Haas *et al.* (2013) of *N. glauca* gene expression data published by Long *et al.* (2016). Based on this assembly, genes were aligned, and their differential expression was analyzed. These data were then used to define conditions of epidermis enrichment and drought induction, and contigs in which at least three conditions were met (e.g. adaxial epidermis enrichment, abaxial epidermis enrichment, and adaxial epidermis drought induction) were searched using BLASTX against the National Center for Biotechnology Information (NCBI) nonredundant protein sequence database to find their closest homologs. Sequencing data may be found in the NCBI Sequence Read Archive under accession no. PRJNA765497.

Wax and cutin monomer profiling using gas chromatography–mass spectrometry

Epicuticular wax extraction was performed by chloroform dipping, as described previously (Alcerito *et al.*, 2002; Bourdenx *et al.*, 2011; Roth-Nebelsick *et al.*, 2013; Simpson & Ohlrogge, 2016; Lange *et al.*, 2019) and by mechanical extraction using gum arabic. In both cases, wax composition was profiled by gas chromatography–mass spectrometry (GC–MS) as described in Cohen *et al.* (2019). See Methods S1 for details and validation of the extraction methods.

Leaf desiccation assays and whole-plant drought trials using a lysimetric system

Cuticular water loss rates were measured in detached leaves of wild-type (WT) and mutant lines by weighing and extrapolating water loss once this had reached the linear phase as described in Cameron *et al.* (2006). For details, see Methods S1. Drought trials carried out using a lysimetric system were performed in either soil (2018 and 2019) or sand (2020) as described in Halperin *et al.* (2017) and Dalal *et al.* (2020) (see Methods S1 for details). In short, plants were grown on the lysimeter system for a period before drought, when biomass accumulation and water use efficiency (WUE) were monitored. Following this, irrigation was reduced to 50% of the previous day transpiration (i.e. if a plant transpired 300 ml, it would receive 150 ml during the following night's irrigation). Once each plant reached the transpirational

threshold, set to 20% of the average daily transpiration on the last day before drought initiation, it received no irrigation for an additional 2 d after which irrigation was resumed in excess.

Stomatal analysis and scanning electron microscopy

Stomatal imprints were taken from adaxial and abaxial epidermises of glasshouse-grown plants, as described in Yaaran *et al.* (2019). See Methods S1 for a detailed description.

Photosynthetic efficiency and light response

Photosynthetic efficiency was assessed by measuring gas exchange at rising CO_2 concentrations ('A/C_i curves'), using an LI-6800 portable photosynthesis system (Li-Cor Inc., Lincoln, NE, USA). Light response was assessed by measuring gas exchange at rising light intensities using the LI-6800 portable photosynthesis system. For details and exact parameters used in each program, see Methods S1.

Statistical analysis

The JMP 14 and 16 software (SAS Institute; http://www.jmp.com/en_us/home.html) were used for all statistical analyses, except for two-piece linear curves in the drought experiments in which SPAC-ANALYTICS software (https://www.plant-ditech.com/products/spac-analytics) was used to find the best fitting regression lines. A Student's *t*-test was used when comparing the 15 lines to WT and Dunnett's test when representative lines were compared with WT. Mutants were always compared with WT, except in the spring drought trial where Tukey's HSD test was used, and all groups were compared. Regression line nonzero slope was assessed by an *f*-test using PRISM 7 software (GraphPad, San Diego, CA, USA).

Results

Transcriptomics of *N. glauca* adaxial and abaxial epidermal tissues under drought conditions facilitates the discovery of cuticular lipid-related genes

To generate a population of cuticular lipid metabolism mutants in *N. glauca*, it was first essential to identify cuticular lipid-associated genes that are active in the *N. glauca* epidermis layer. We thus performed transcriptome analyses of five different shoot tissues, including dissected adaxial and abaxial leaf epidermis, stem epidermis, entire leaves, and whole stems. Expression profiling was carried out in both well-watered plants and ones under drought conditions. We next mined the transcriptome dataset for transcripts that were epidermis-enriched, drought-induced, or a combination of the two. Many homologs of cuticular lipid metabolism genes (e.g. *KCS6*, *CER1*, *FAR*, and *ABCG32*) displayed a similar 'expression signature', high epidermal enrichment, and mild drought induction (Figs 2, S2). Out of tens of genes

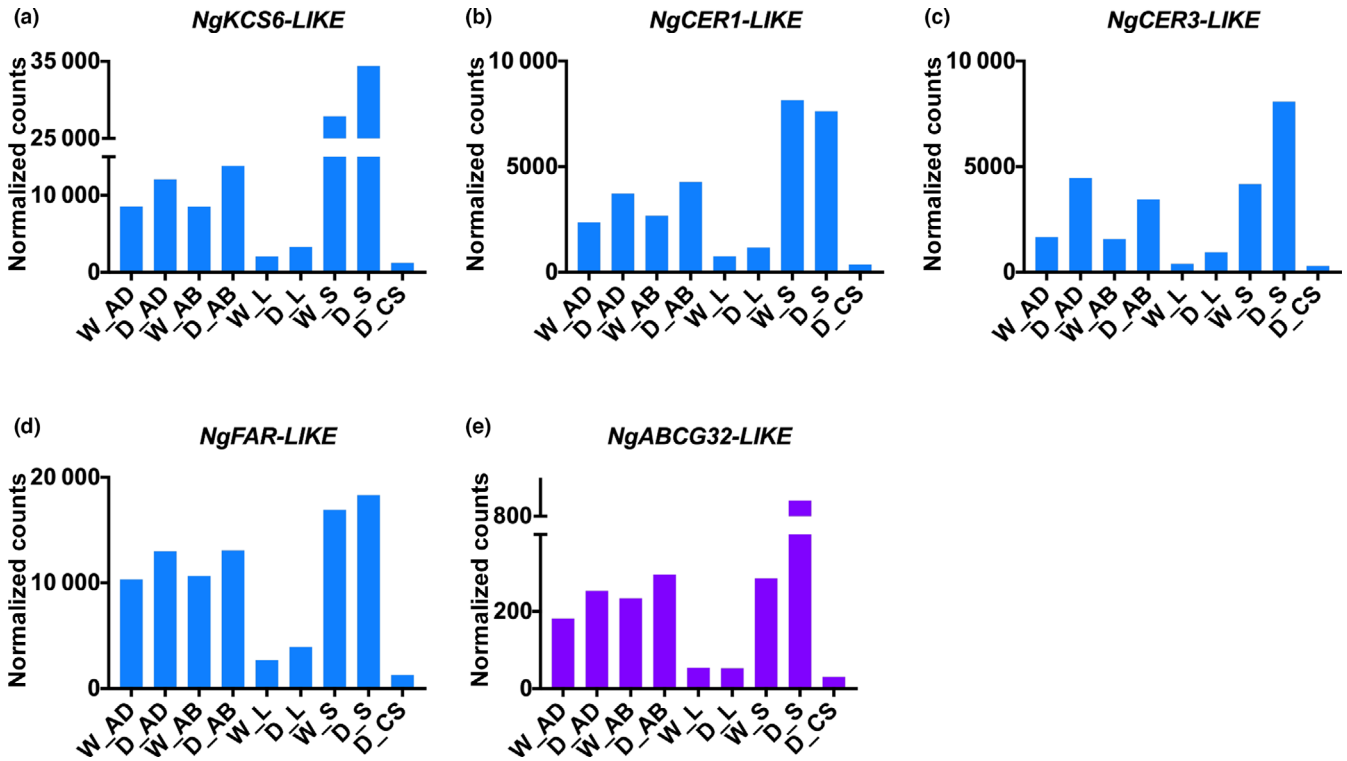

Fig. 2 Epidermis-enriched and drought-induced expression of *Nicotiana glauca* genes showing homology to known cuticular lipids genes from other species. For each sample, three biological replicates of each tissue, grown under either well-watered conditions or drought-treated, were collected and pooled to reduce variance. Wax synthesis genes are indicated in blue (a–d) and the transporter gene in purple (e). AB, abaxial epidermis tissue; AD, adaxial epidermis tissue; CS, complete stem; D, drought-treated plants; L, whole leaf tissue; S, stem epidermis tissue; W, watered plants.

Table 1 Sixteen genes targeted for knockout mutations in *Nicotiana glauca* in this study, their function, and Arabidopsis homologs.

Gene	Function	Role	Arabidopsis homolog
NgSHN1-like	Transcription factor	Regulates wax and cutin synthesis	*AtSHN1* – AT1G15360
NgSHN3-like	Transcription factor	Regulates wax and cutin synthesis	*AtSHN3* – AT5G25390
NgMYB96-like	Transcription factor	Regulates wax synthesis in response to drought	*AtMYB96* – AT5G62470
NgGPAT4-like	Cutin synthesis	Attaches cutin monomers to glycerol	*AtGPAT4* – AT1G01610
NgCYP86A22-like	Cutin synthesis	ω-Hydroxylates cutin monomers	*AtCYP86A7* – AT1G63710
NgGDSL-like	Cutin synthesis	Polymerizes cutin monomers	*AtGDSL* – AT1G75900
NgLACS-like	Wax and cutin synthesis	Converts fatty acids to acyl-CoA and *vice versa*	*AtLACS1* – AT2G47240
NgKCS6-like	Wax synthesis	Part of the fatty acid elongase complex	*AtCER6* – AT1G68530
NgCER1-like	Wax synthesis	Together with *CER3*, converts acyl-CoA to alkanes	*AtCER1* – AT1G02205
NgCER3-like	Wax synthesis	Together with *CER1*, converts acyl-CoA to alkanes	*AtCER3* – AT5G57800
NgMAH1-like	Wax synthesis	Hydroxylates alkanes to form secondary alcohols and ketones	*AtMAH1* – AT1G57750
NgFAR-like	Wax synthesis	Reduces acyl-CoA to form primary alcohols	*AtCER4* – AT4G33790
NgWSD1-like	Wax synthesis	Combines fatty alcohols and fatty acids to form wax esters	*AtWSD1* – AT4G33790
NgABCG11-like	Wax and cutin monomer transport	Transports cutin monomers to the extracellular matrix	*AtABCG11* – AT1G17840
NgABCG32-like	Wax and cutin monomer transport	Involved in cutin transport to the extracellular matrix	*AtABCG32* – AT2G26910
NgACBP-like	Wax and cutin monomer transport	Involved in lipid transport	*AtACBP1* – AT5G53470

putatively associated with cuticular lipids metabolism, we selected 16 for further study. Mutating these genes could alter wax and cutin synthesis and transport in a variety of manners, resulting in a set of mutant lines with diverse wax compositions (Table 1). We next generated plant transformation vectors for editing the 16-gene set through CRISPR-Cas9 technology and introduced them to *N. glauca* (Fig. S1).

Cuticular lipid mutants display diverse surface and morphological phenotypes

Of the 16 genes targeted, 10 exhibited visual surface-related phenotypes in the T0 generation (Figs 3, S3). These included glossy leaves and stems and fused anthers in the *kcs6* mutant alleles, glossy leaves and stems in the *far* and *cer1* mutants, and glossy leaves alongside waxy stems in *cer3* mutants (Fig. 3). The *abcg11* mutant, the only line that never flowered (even after 3 yr), possessed small, glossy, crinkled, brittle leaves. Both *cyp86a22* and *abcg32* showed elongated and malformed leaves, whereas *gpat4* displayed elongated leaves and leaf fusions. Mutants in *GDSL* were small with elongated and malformed leaves. Finally, the *lacs* mutants displayed both a glossy phenotype and leaf deformities (Fig. S3). Sequencing the amplicons covering the targeted edit sites revealed a wide range of mutations, from single base-pair insertions or deletions, deletion of a triplet coding for a single amino acid to a 200-bp deletion (Fig. S1). First-generation plants (i.e. T0) possessed homozygous, hemizygous, or heterozygous mutations.

Surface wax composition and crystal morphology in wax gene mutants

Out of the 10 mutants, we focused the study on four wax metabolism genes and the *abcg32* mutant that served as a control, as it is affected in cutin monomer transport. We next extracted leaf epicuticular wax by either chloroform dipping (Figs 4, S4; Table S1) for 15 s or by mechanical removal using gum arabic (Figs S5, S6). These two extraction methods resulted in similar results when epicuticular wax composition was analyzed using GC–MS (see ratio in Fig. S7). Wax composition in *N. glauca* is typically dominated by a C_{31} alkane (92% according to Mortimer *et al.*, 2012) along with C_{33} alkanes, C_{24}, C_{26}, and C_{28} fatty alcohols, and smaller amounts of C_{26} aldehydes (as well as trace amounts of other alkanes, alcohols, aldehydes, and fatty acids). Mutations in different genes had a drastic effect on epicuticular wax composition (Figs 4, S4–S6). Leaves of *kcs6* reduced wax components with a chain length above 26 carbons almost completely, making them nearly free of alkanes (Figs 4a, b, S4A–D, S5A,B, S6A–F) while accumulating shorter chain length waxes such as C_{18}, C_{20}, C_{22}, and C_{24} alcohols (Fig. 4c–f), and C_{24} aldehydes (Fig. S6I). Leaves of the *cer1* mutants reduced the abundance of all alkanes (Figs 4a,b, S4A–D, S5A, B, S6A–F) and significantly increased very long-chain aldehyde (Fig. S6L,M) and VLCFA abundance (Fig. S6P,Q). *cer3* mutants had a significant reduction (*c.* 80%) in their C_{31} alkane load although C_{33} alkanes showed a trend of increase that was significant in one line (Figs 4a,b, S5). The *far* mutants displayed extremely reduced fatty alcohol (Fig. 4c–f) and C_{26} and C_{28} aldehyde (Fig. S6J,K) content, contrasted by a trend or significant increase in their alkane load (Figs 4a,b, S6B,C). In the *abcg32* mutants, wax composition was similar to that of WT, with only a trend of reduction in C_{31} alkane load (Fig. 4a) and other minor changes.

Alterations in the composition of epicuticular waxes had a strong effect on wax crystal morphology, as visualized using cryo-SEM (Fig. 5). The typical wax crystals of *N. glauca* leaves are of dense rodlets (Fig. 5a). In *cer1* leaves, a thin layer of flakes replaced the wax rodlets (Fig. 5b). Leaves of *cer3* displayed crystal morphology similar to that of WT. However, these crystals were reduced in size and more sparsely distributed (Fig. 5c). Leaf wax of *kcs6* lost its rodlet-like morphology and appeared as structured lines of vertically positioned membranous platelets (Fig. 5d). The *far* leaves exhibited large vertical sharp-edged plates, which were sparsely distributed (Fig. 5e). Finally, the *abcg32* mutant wax crystals appeared normal as expected from its almost unaltered wax composition (Fig. 5f).

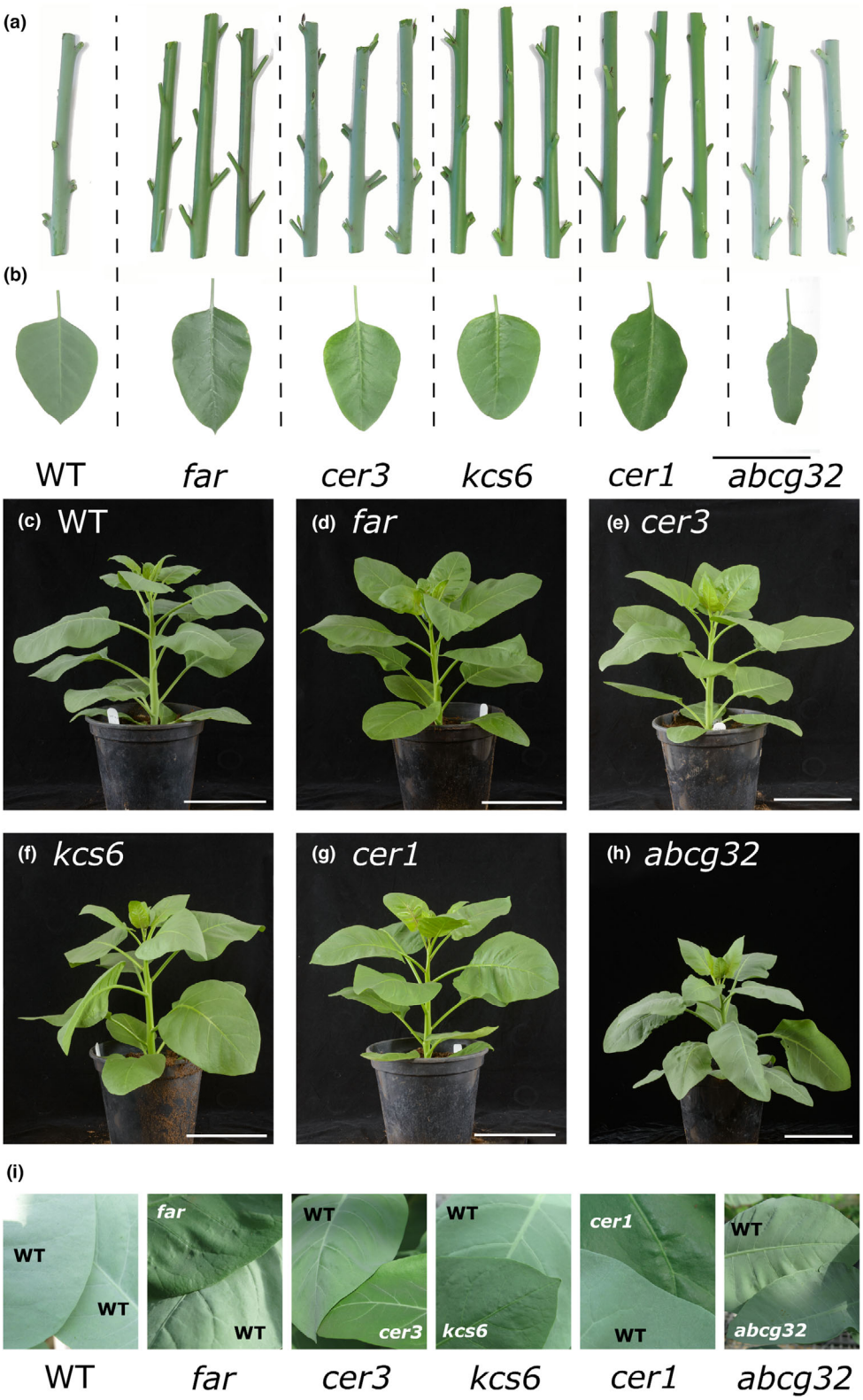

Fig. 3 Plant surface phenotypes of mutant *Nicotiana glauca* plants analyzed in this study. (a) Representative stems of wild-type (WT) and the 15 independent mutant lines from the five genes investigated in depth. (b) Representative leaves of WT and mutant plants. Bar, 5 cm. (c–h) Representative whole plants. Bar, 15 cm. (c) WT; (d) *far*; (e) *cer3*; (f) *kcs6*; (g) *cer1*; (h) *abcg32*. (i) Images of WT leaves adjacent to mutant leaves.

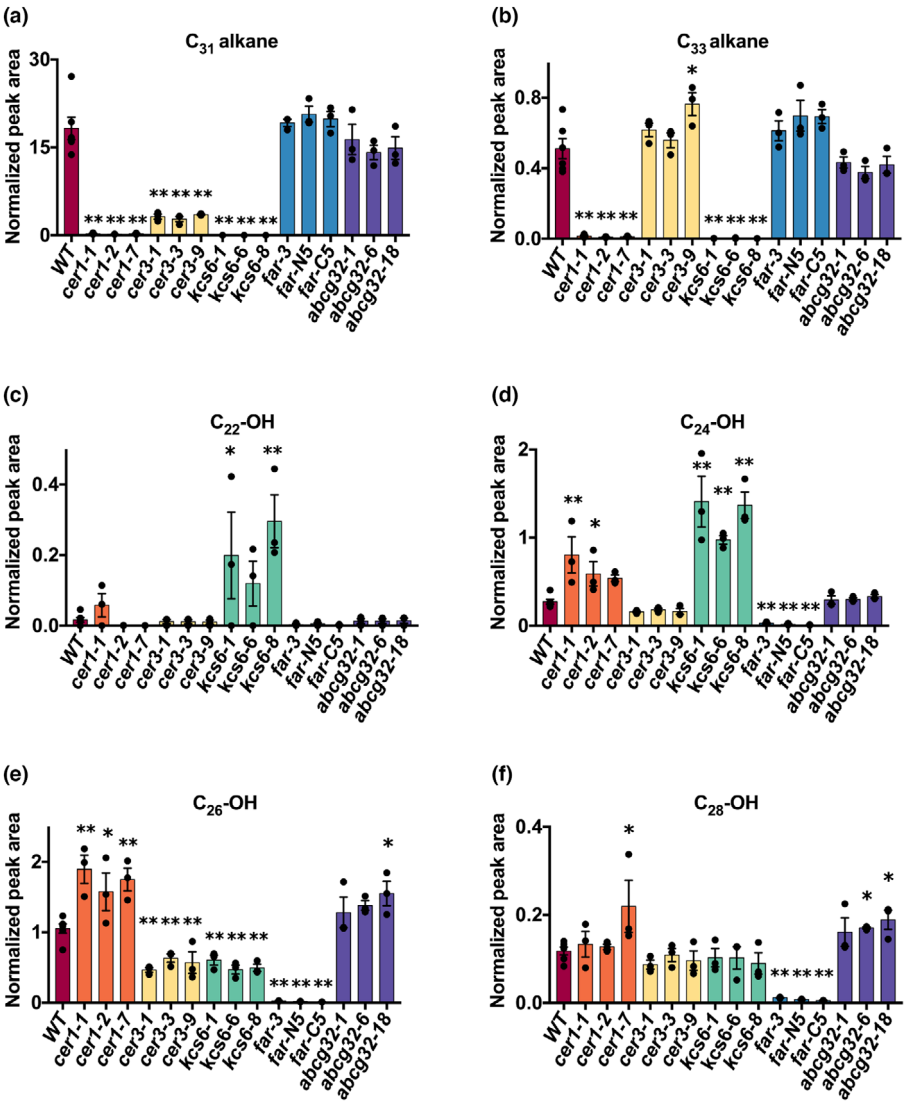

Fig. 4 Relative abundance of major wax components in *Nicotiana glauca* leaves. (a, b) Alkanes and (c–f) primary alcohols. Numbers indicate carbon chain length. Independent mutant alleles of the same gene are indicated by the same color. Wild-type (WT), $n = 6$; all other lines $n = 3$. Black circles indicate individual results. *, $P < 0.05$ and **, $P < 0.01$ as determined in comparison with WT (Student's *t*-test). Bars, ±SE. Wax components were extracted in chloroform, derivatized, and quantified by gas chromatography–mass spectrometry.

Cutin composition of wax metabolism mutants

Wax metabolism and cutin metabolism share some common enzymes and precursors. We therefore examined the cutin composition in the mutant set (Fig. S8 and the entire monomer profiling in Table S2). Here, the impact of mutations was far less drastic, as compared to their effect on wax composition, and very distant from the reduction percentage of the stronger wax mutants (98.8–98.3% in *cer1* lines and 99.9% in *kcs6* lines comparing C_{31} alkanes to WT and 96.3–93.2% in all fatty alcohols in *far* lines). This was not the case for the *cer1* lines showing a significantly altered load of several cutin monomers and reaching a reduction of *c.* 64% in methyl caffeate abundance (Fig. S8A–H). Furthermore, when we analyzed the data per chemical class, we found that *cer1* mutants had a significantly lower fatty acid load in two out of three lines (Fig. S8B) but significantly higher levels of ω-hydroxylated fatty acids (Fig. S8C). In addition, *cer1* cutin had a significantly higher content of VLCF alcohol and a reduced content of total phenolic compounds (Fig. S8E).

Reduction in alkane abundance increases cuticular water loss drastically

In this study, we examined both the loss of water through the cuticle itself (with no stomatal water loss), using excised leaves, and intact leaf transpiration, including all forms of water loss in whole plants. To examine how changes in chemical composition affected the physiological state of mutant plants, we analyzed cuticular water loss. Leaves were detached from plants and weighed every 2 h once they reached the linear weight loss stage. The *cer1* mutants were most strongly affected out of the five mutant genotypes, showing threefold water loss rate (Fig. 6a). The *kcs6* mutant leaves also showed a higher water loss rate, whereas *abcg32* leaves displayed a slight but significant increase. Surprisingly, of the *cer3* mutant lines, only *cer3-1* lost water significantly faster. By contrast, two of the three *far* lines lost water significantly slower than WT leaves (Fig. 6a).

Next, we plotted the detached leaf water loss rate against the average abundance of wax and cutin components in independent

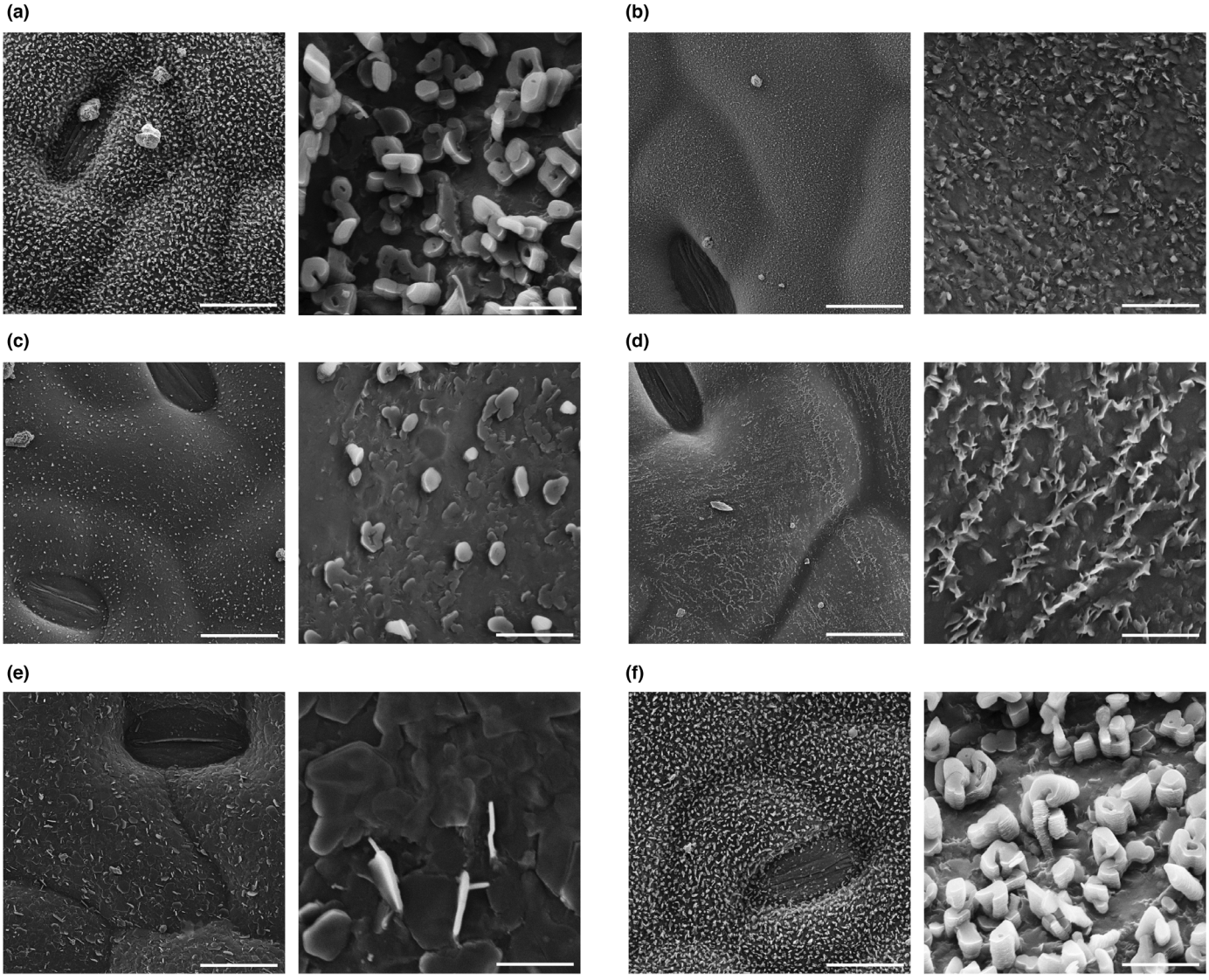

Fig. 5 Cryo-SEM images of wax crystal dispersion and structure on the adaxial side of mutant *Nicotiana glauca* plants. (a) Wild-type leaf; (b) *cer1* leaf; (c) *cer3* leaf; (d) *kcs6* leaf; (e) *far* leaf; (f) *abcg32* leaf. For each line, a magnification of ×2500 with a 20 μm bar is shown on the left and ×25 000 with a 2 μm bar is on the right.

mutant lines (Fig. 6b–f). We found a correlation with an R^2 of 0.786 between water loss rate and total alkane content (slope = −4.8). Yet, *cer3* leaves lost water at a slower rate than their alkane content would predict, while *cer1* plants lost water at a faster rate than that predicted by the linear regression (Fig. 6b). When cutin components were plotted against water loss, a positive correlation (R^2 = 0.718, slope = 0.09) was found with total cutin lipids, although the differences in the cutin component abundance were far smaller between different lines compared to those in wax components (Fig. 6d). By contrast, phenolic compounds found in the cutin fraction (R^2 = 0.616, slope = −0.06; Fig. 6f), especially methyl caffeate (R^2 = 0.66, slope = −0.06), were negatively correlated with water loss. Although the role of the phenolics is not clear to us, these results highlight that alkanes in the epicuticular wax fraction play an important role in preventing cuticular water loss. To ensure that the factor affecting water loss rates was not the total wax load, we plotted these two factors. Here, the R^2 was 0.722 (slope = −4.3; Fig. S9A), showing that adding the alcohols to the correlation reduced rather than increased its predictive strength. For further validation, we plotted the total wax of *kcs6* and *cer1*, in which fatty alcohols are the major wax component, against water loss. Here, similar to the fatty alcohols' correlation, a positive correlation was seen (R^2 = 0.63, slope = 0.73; Fig. S9B), that is, a higher wax load correlating with faster water loss, exemplifying once more that alkanes alone and not the total wax load are correlated with reduced water loss.

Wax has little effect on water loss predrought, but alkanes are essential for recovery from drought, as they prevent drought-induced leaf death

The major effect of epicuticular wax mutations on cuticular water loss led us to hypothesize that under well-watered conditions,

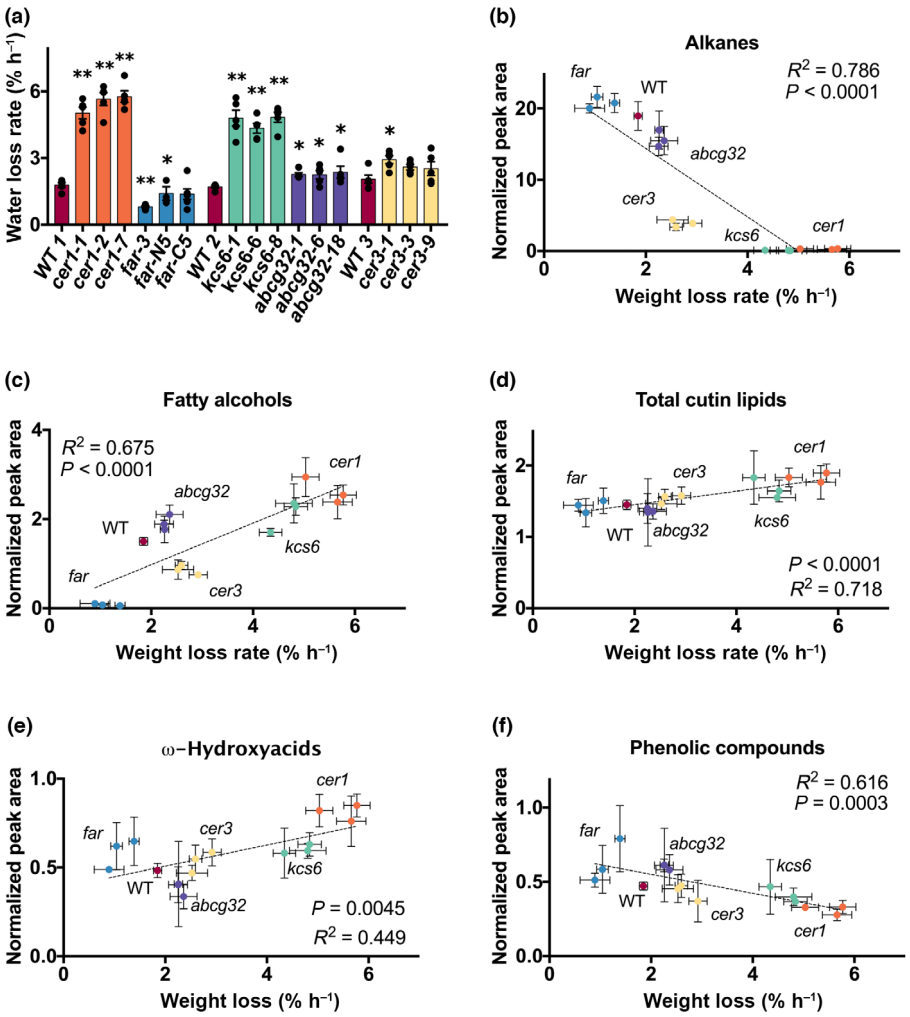

Fig. 6 *Nicotiana glauca* cuticular water loss rate and its correlation with different wax and cutin components. (a) Cuticular water loss rate. The experiment included three assays during consecutive days, each with its own wild-type (WT) samples (WT1–WT3). Mutant alleles of the same gene are indicated in the same color. Black circles indicate individual results. *, $P < 0.05$ and **, $P < 0.01$ (Student's *t*-test); $n = 5$. Bars, ±SE. Correlation between water loss rate and (b) sum of all alkane wax components; (c) sum of very long-chain fatty alcohols; (d) sum of all lipidic components of the cutin monomers; (e) sum of ω-hydroxylated fatty acids of the cutin monomers; and (f) sum of all phenolic compounds of the cutin monomers. R^2 indicated in each correlation graph is generated from the average water loss rate and average abundance of the different wax and cutin components in the same independent mutant line, obtained in separate experiments. Bars, ±SE.

plants with greatly reduced alkane abundance would transpire at higher rates and be more susceptible to drought. We tested this hypothesis using a weighing lysimeter system, in which plants are weighed every 3 min and in combination with environmental measurements (e.g. temperature, humidity, and light intensity) performed in parallel, transpiration, stomatal conductance (g_s), biomass accumulation, WUE, and drought response can be extrapolated. The first two experiments performed with this system in the summer and winter seasons involved two and three different mutant alleles of *cer3*, respectively. To our surprise, in the first, summer experiment (Fig. S10), *cer3* plants had almost identical transpiration compared with WT pre (Fig. S10A,D), during (Fig. S10B,E), and post (Fig. S10F) drought. In the 'winter' experiment (Fig. S11), we observed *cer3* transpiration was similar to that of WT pre- (Fig. S11A,D), during (Fig. S11B,E), and post-drought (Fig. S11C,F). Furthermore, *cer3* biomass accumulation was not impaired in both experiments (Figs S10G–I, S11G,H), as was their WUE (Figs S10J, S11I). Plants that respond to drying soil by closing their stomata at a higher soil water content (theta point) are more likely to show drought tolerance. In the 'summer' experiment, *cer3* lines had a theta point similar to that of WT (Fig. S10K), whereas, in the 'winter' experiment, their theta point was at a significantly higher soil water content (Fig. S11J). The results indicated that *cer3* mutants had a response similar to that of WT plants despite their reduced wax load both under well-watered and drought conditions, and those differences which did exist were correlated with higher drought resistance.

The findings described above prompted us to examine whether those lines with the most drastically reduced wax load (above 90% reduction in alkanes/fatty alcohols) of our mutant set would behave similarly. We therefore performed an additional experiment during the spring. In this 'spring' experiment, we placed three different mutant alleles of either *cer1*, *kcs6*, or *far* on the lysimetric system alongside three lines of WT plants. Similar to the *cer3* results, under well-watered conditions, there was no significant difference between the mutants and WT plants in daily transpiration (Fig. 7a), transpiration rate (Fig. 7d), plant growth rate (Fig. 7g), and WUE (Fig. 7j).

Once we exposed well-watered plants to drought and recovery (i.e. rewatering), we detected a markedly different response in the wax mutants. *cer1* mutant lines' theta point was significantly lower than that of WT (Fig. 7k), leading to *cer1* plants having a significantly higher transpiration rate throughout extended periods of the day during drought that was not observed in the other mutant lines, which had a theta point similar to that of WT

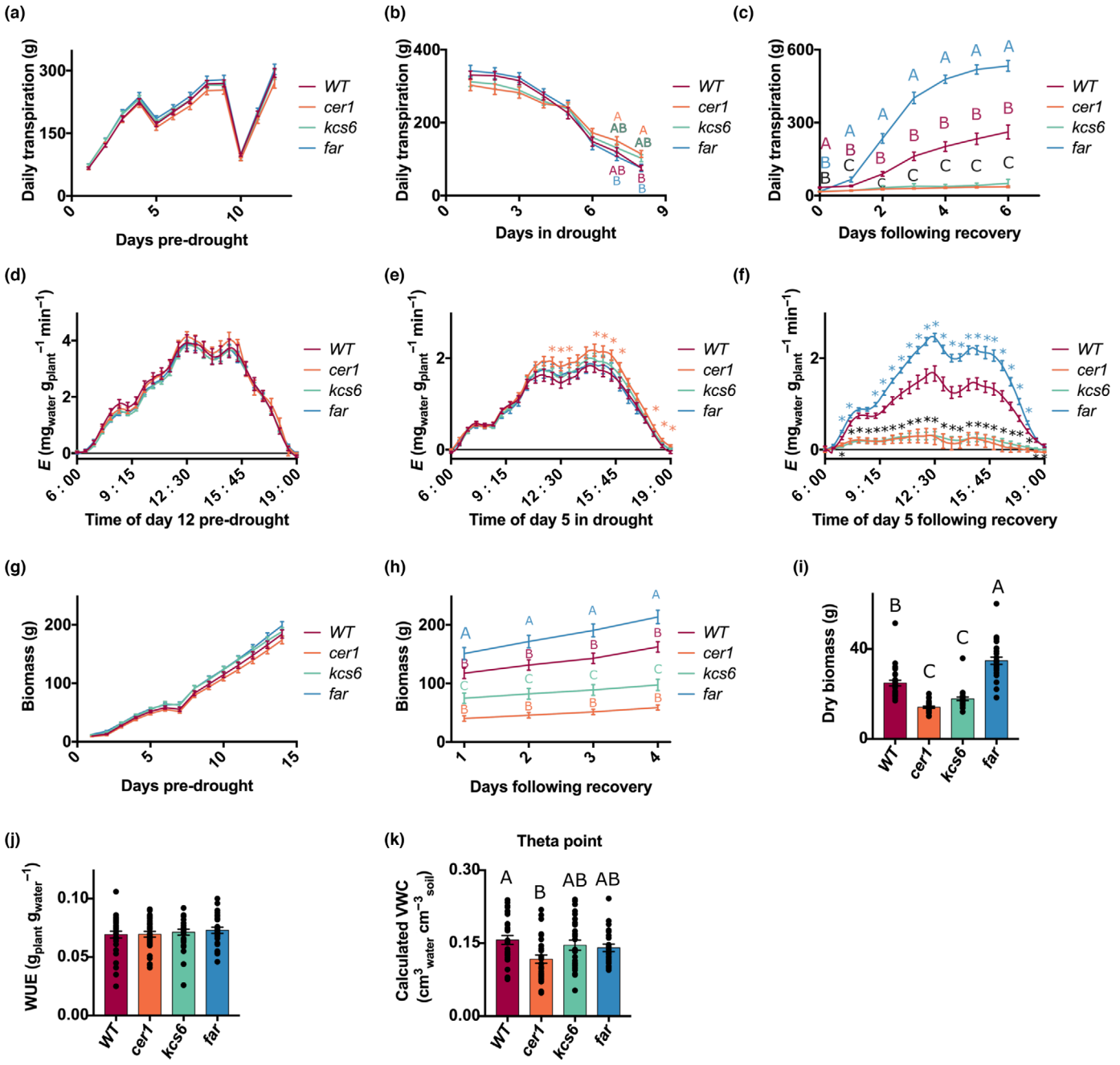

Fig. 7 Multiparameter analysis of mutant *Nicotiana glauca* plants assayed in a lysimetric system and assayed following full irrigation, drought, and recovery. (a) Predrought daily transpiration. (b) Daily transpiration following drought initiation and before recovery. (c) Daily transpiration following recovery. Since each individual plant received full irrigation 3 d after it transpired below a 20% daily transpiration threshold (see the Materials and Methods section), the days in recovery are different for each individual plant and averaged according to the number of days postirrigation renewal per plant. (d) Transpiration rate during day 12 before drought induction. Measurements were taken every 3 min, though error bars are only shown every 30 min. (e) Transpiration rate during the fifth day of drought. (f) Transpiration rate during the fifth day after plant recovery, averaged from different dates for each plant according to its recovery date. (g) Plant biomass during the period before drought induction. (h) Plant biomass during 4 d before the experiment ended, at which time all plants had been recovered. (i) Dry shoot biomass at the experiment end. (j) Water use efficiency (WUE) as calculated predrought. (k) 'Theta point' volumetric water content (VWC) at which plants began reducing transpiration rate in response to drying soil. All data are the average of three independent mutant alleles used in this experiment, including wild-type (WT), which had three independent lines grown first in tissue culture before transferring to the glasshouse. The following number of plants was analyzed: WT $n = 28$–33; *cer1* $n = 27$–31; *kcs6* $n = 25$–29; *far* $n = 24$–26. Black circles indicate individual results. Different letters indicate a significance of $P < 0.05$ as determined in a Tukey's HSD test. *, $P < 0.05$ compared with WT (Student's *t*-test). Asterisks are placed above SE lines (bars), though points are significant for every point measured between the bars. Bars, ±SE.

(Fig. 7b,e). Though the increase in *cer1's* transpiration rate is significant, the effect size is relatively small and reached an *c.* 20% increase during the afternoon hours. This was not the case following recovery. At this phase, it was apparent that, whereas *cer1* and *kcs6* plants lost many leaves following drought treatment, WT and to an even greater extent *far* mutants retained their leaves, leading to a greater transpiring surface area and elevated transpiration (Fig. S12). *far* plants' daily transpiration was significantly higher than WT plants, which exhibited significantly greater transpiration than *cer1* and *kcs6* (Fig. 7c,f). These differences increased with time up to the sixth day following resumption of irrigation; *far* plants transpired 533 ml a day on average, WT 262 ml, *kcs6* 50 ml, and *cer1* transpired only 36 ml on average during that day (Fig. 7c). These results were mirrored by the transpiration rate (Fig. 7f), plant growth rate (Fig. 7h), and shoot dry biomass (when the experiment ended; Fig. 7i). The combination of these results points to alkanes protecting leaves from drying during drought. Thus, following recovery, plants with an elevated alkane abundance were able to reopen stomata and resume carbon assimilation. By contrast, alkane-deficient plants had to produce completely new leaves to return to previous assimilation rates.

Drought followed by recovery leads to stem cracking

Toward the completion of the weighing lysimeter experiment, we detected an intriguing phenotype, which has not been reported in the context of wax deficiency to the best of our knowledge. Sixteen out of 27 *kcs6* lines derived from all three independent mutant alleles displayed severe cracks along their stems penetrating the xylem and deep into the stem pith (Figs 8a,b, S13A,B). Intriguingly, these cracks even led to sap dripping freely out of the xylem and cracks (Figs 8a, S13A). Besides the *kcs6* plants, there was one occurrence of stem cracking in a *cer1-1* plant, indicating that the occurrence in *kcs6* plants was not an isolated event. When investigating the reasons for the *kcs6* stem phenotype, we found that the 11 *kcs6* plants with intact stems whose noncracking phenotype was not due to technical reasons, such as small plants not reaching drought, had a similar biomass and theta point compared with the plants with cracked stems at the onset of drought (Fig. S13E,F). While all 16 cracked plants were recovered during 3 d, from the 13th to the 15th day of drought, the uncracked plants were recovered between the 10th and the 18th day of drought. When examining the 11 *kcs6* plants with undamaged stems, we found that they reduced their volumetric water content at a rate similar to those with cracked stems (Fig. S13G). Thus, as is seen from the broader range of drought duration before recovery, plants that depleted their water and recovered rapidly, as well as those that transpired less and were exposed to drought more gradually, did not experience stem cracking.

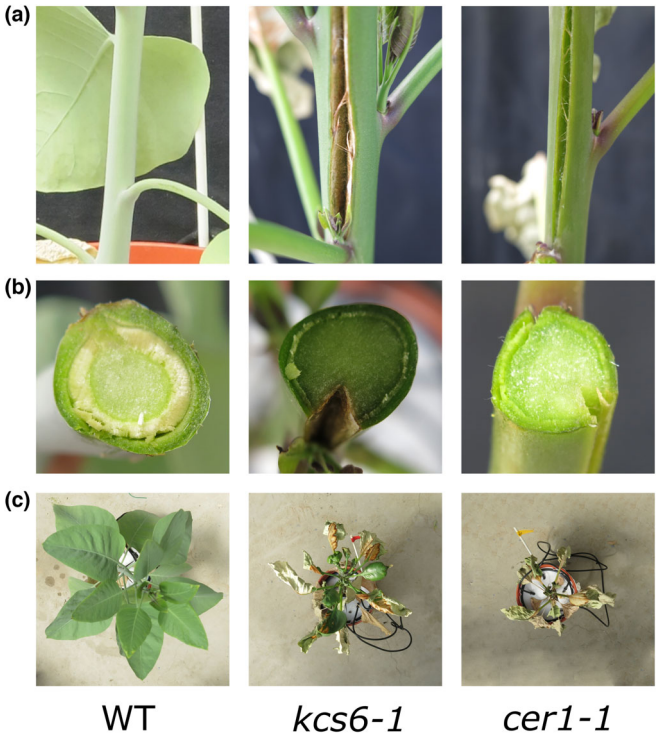

Fig. 8 *Nicotiana glauca* stem cracking phenomenon. (a) Images of cracked stem phenotypes in *kcs6* and *cer1* mutants and a representative wild-type (WT) stem. (b) Images of cut stems showing the radial formation of the crack through the xylem and into the stem pith cells. (c) Whole plants photographed from above and displaying differential drought response.

Stomatal aperture and development do not compensate for elevated cuticular water loss

We next examined whether the discrepancy between high leaf cuticular water loss and normal transpiration rate under well-watered conditions was related to a reduced stomatal density, size, or aperture, leading to the elevated cuticular water loss being compensated for by reduced stomatal water loss. However, all mutants had similar stomatal density (Fig. S14A,D) and sizes (Fig. S14B,E) compared with WT, and even those insignificant differences in density were compensated for by larger stomata; that is, a significant negative correlation existed for stomatal density and stomatal size (Fig. S15). Abaxial stomatal aperture (Fig. S14C) was the only parameter where we found a significant difference, with *cer1* having a larger stomatal aperture, while all other stomatal apertures were similar to those of WT (Fig. S14C, F). Thus, unlike our original hypothesis, cuticular water loss was not compensated for by stomatal aperture or morphology.

The glossy phenotype of wax mutants does not significantly affect light response and photosynthetic efficiency

Despite extreme differences in their wax composition, *cer1*, *cer3*, *kcs6*, and *far* mutants all displayed a glossy leaf appearance. To examine whether this phenotype affects photosynthetic efficiency, we measured RUBISCO efficiency (Vc_{max}) and maximal electron transport rate (J_{max}) by monitoring the carbon assimilation while the substomatal CO_2 concentration was raised (A/C_i curves). The *cer1* mutant lines appeared different from all other mutants and WT as their A/C_i curve plateaued much earlier than all other

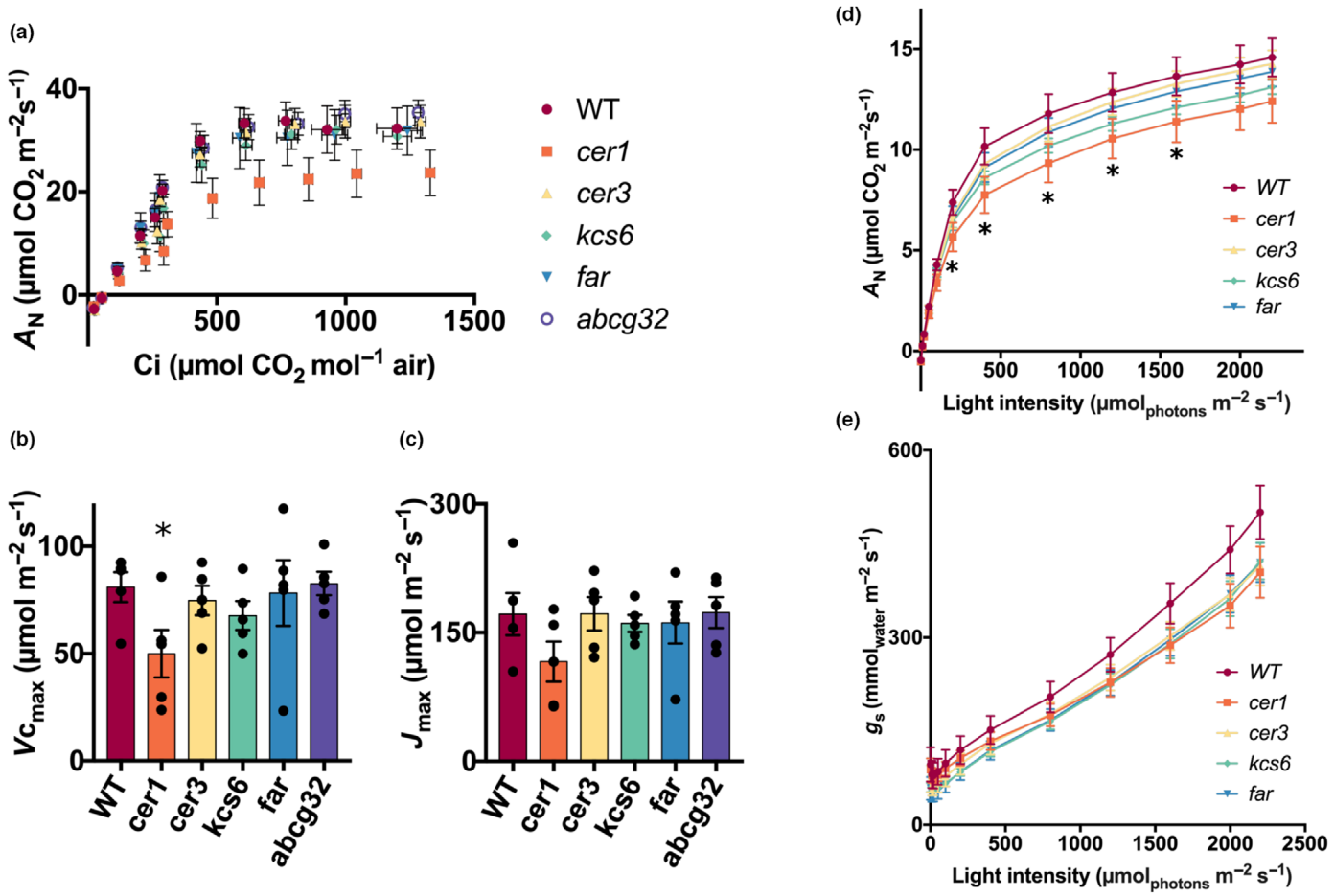

Fig. 9 Photosynthetic efficiency and effects of wax deficiency on gas exchange in response to rising light intensity of wild-type (WT) and four *Nicotiana glauca* wax biosynthesis mutant lines. (a) Average carbon assimilation with rising C_i concentrations. (b) Vc_{max}, indicating RUBISCO efficiency. (c) J_{max}, indicating maximal electron transport rate, $n = 5$. (d) Carbon assimilation in response to rising light intensity. (e) Stomatal conductance in response to rising light intensity. $n = 9$. Bars, ±SE. Black circles indicate individual results. *, $P < 0.05$ (Student's *t*-test).

genotypes (Fig. 9a). Although the J_{max} of *cer1* plants was not significantly lower (Fig. 9c), their Vc_{max} was significantly reduced (Fig. 9b). The wax composition of *cer1* mutants is similar to that of *kcs6*, which leads to very similar responses in assays where the wax composition is the underlying factor. However, *cer1* is the only mutant with altered cutin, suggesting that the differences seen in the A/C_i curves resulted from altered cutin but not wax load or composition.

We next asked whether the glossy phenotypes of wax mutants had a significant impact on light responses. Thus, we exposed plants of each genotype to 12 rising light intensities and recorded carbon assimilation and stomatal conductance (Fig. 9d,e). No plants reached photoinhibition along these points, despite reaching a light intensity of 2200 μmol m^{-2} s^{-1} (while plants were grown at an intensity of 100–200 μmol m^{-2} s^{-1}). Similar to the results of the A/C_i curves, *cer1* mutants were the only plants displaying an altered phenotype, exhibiting reduced carbon assimilation at five points of the dozen light intensities measured (Fig. 9d). These results demonstrate that light reflectance by wax crystals does not alter *N. glauca* photosynthetic capacity under nonstressed conditions.

Discussion

Wax biosynthesis in *N. glauca*

In this study, we simultaneously characterized a large number of mutants corresponding to different cuticular lipid genes, filtering out indirect effects, such as changes in cutin composition, and providing insight into the epicuticular wax biosynthetic pathways in *N. glauca*. As reported previously, the *CER1* gene is involved in converting aldehydes to alkanes. This may be seen in the drastic reduction in the alkanes in *cer1* mutants and the accumulation of C_{32} and C_{34} aldehydes; compounds expected to be decarboxylated to form the most abundant C_{31} and C_{33} alkanes. By contrast, *far* mutants have an extreme reduction in C_{26} and C_{28} aldehydes. This finding implies that unlike *CER1*, the *FAR* gene is responsible for the synthesis of these shorter aldehydes in addition to fatty alcohol synthesis. Another intriguing result is the wax composition of *cer3*. Although CER3 was suggested to participate in alkane production along with CER1, our results show that *cer3* plants have reduced $C_{29–31}$ alkane load, unaffected C_{32} alkane load, and an increase in C_{33} alkanes. The increase in C_{33}

alkanes in *cer3* mutants could be explained by analogy to the Arabidopsis *CER1* gene, which has several homologs that are responsible for the synthesis of alkanes of different lengths (Pascal *et al.*, 2019). Indeed, when analyzing the transcriptomic data, four *CER3* homologs were found, two of which had high expression levels. Of these, one displayed leaf epidermis and high stem epidermis expression (Fig. S16A), explaining the reason for *cer3* mutant glaucous stem. By contrast, of four *CER1* homologs, only the silenced gene displayed high expression levels in leaves (Fig. S16D).

Alkanes reduce cuticular water loss, but cutin affects photosynthetic efficiency and light response

Both *cer1* and the *kcs6* mutants possess an extremely reduced alkane load. Nevertheless, *cer1* also exhibits an altered cutin composition, with significantly less phenolic compounds and more ω-hydroxylated fatty acids. Comparing the phenotype of *cer1* to that of *kcs6* enabled us to make this distinction. Cuticular water loss is affected when both genes are mutated, although the rate is higher in *cer1* mutants. Here, we detected an additive effect of altered cutin, despite the major effect being derived from reduced alkane abundance. Effects that are only present in *cer1* and not *kcs6* that we attribute to cutin are the reduced Vc_{max} and lower carbon assimilation with rising light intensity. However, since these conclusions were drawn from a single cutin mutant, further investigation is necessary with additional cutin mutants to validate cutin's effects on photosynthetic efficiency and light response.

Cameron *et al.* (2006) showed that the overall accumulation of epicuticular waxes following exposure to drought in *N. glauca* reduced the rate of cuticular water loss. However, the drought response in *cer1* and *kcs6* plants was nearly identical, suggesting that alkane abundance is a major factor preventing leaf death during drought and hastening recovery upon re-irrigation. While the correlation of alkanes with the water loss rate is high, it does not seem to be linear. The *cer3* mutants possess an *c.* 20% of the WT C_{31} alkane load and had only a slight increase in their water loss rate. It therefore seems that although alkanes reduce cuticular water loss, the threshold amount required for having a protective effect may be well lower than the alkane abundance in WT *N. glauca* plants.

Alkane abundance is essential for leaf retention following drought, leading to accelerated recovery, but does not reduce transpiration under well-watered conditions

Following the results of the detached leaf cuticular water loss assay, we anticipated that the mutant plants would transpire at a higher rate under well-watered conditions. This is in line with many studies reporting epicuticular wax conferring drought tolerance, achieved in many cases due to reduced transpiration (reviewed in Xue *et al.*, 2017). Our conclusions from three independent whole-plant growth and drought experiments indicate that drought tolerance is achieved by the ability to prevent cuticular water loss once stomata have closed during severe drought. Plants from our mutant collection, regardless of the metabolic impact of the mutation, all transpire and accumulate biomass at a rate similar to that of WT under well-watered conditions. The discrepancy between increased cuticular water loss and similar whole-plant transpiration may be explained by the high transpiration rate during afternoon hours, which reached *c.* 24% per hour of the total plant weight (Fig. 7d) and was primarily due to stomatal transpiration. Furthermore, although *cer1* responded to drought by reducing stomatal conductance at a lower soil water content (a phenotype associated with reduced drought tolerance; Negin & Moshelion, 2017), such a response was not detected in *kcs6* plants. In contrast to the similarity under well-watered conditions, the mutants' recovery dynamics were very different. Here, extreme differences could be seen between plants, clustering according to their wax composition. We found that leaf survival was the underlying phenotype that determined whether plants would recover transpiration and growth rapidly following irrigation resumption (Fig. S12).

In our drought assay, soil water content and transpiration were continually monitored, and plants were recovered once they had reached the same transpirational threshold. By contrast, many previous studies have assayed drought by stopping irrigation for a similar duration of time. This causes plants with higher well-watered transpiration to reach drought conditions earlier and be exposed to drought for a longer period. Furthermore, 'drought tolerance' attributed to altered drought response may, in fact, be secondary to attenuation of other stress conditions. These stress conditions may include high light intensity, temperature, and VPD (Richards *et al.*, 1986). Our experimental setup uncoupled well-watered transpiration and growth from drought response and recovery. This allowed us to determine that the alkane-dependent ability to prevent leaf death under drought by strongly reducing transpiration is essential for recovery.

Changes in wax composition and the stem cracking phenomenon

The phenomenon of stem cracking is known in conifers at the end of the growing season in drought years and increases with drought severity (Zeltiński *et al.*, 2018; Cameron, 2019). However, to the best of our knowledge, it has never been linked to alterations in epicuticular wax abundance or composition. Its appearance in *kcs6* and *cer1* mutants following recovery indicates that stem cracking is indeed alkane-related. The extensive use of annual plants for molecular research of epicuticular waxes has left its effect on perennial and woody plants relatively unexplored. Our study here underscores the use of *N. glauca* as a model system enabling research of wax function in woody species. The exact stage at which stem cracking took place is not clear to us. Even at the end of the drought treatment, we could not detect cracked stems in the *kcs6* plants. However, whether slight initial cracking already started during drought treatment, whether a more gradual recovery would have prevented the cracking, and what threshold of drought conditions results in cracking remains to be determined.

Glossy mutants did not share a common phenotype under the examined conditions

Out of the five mutants examined in this study, four display a glossy phenotype. This striking phenotype appears in plants that lost alkane biosynthesis nearly entirely but also when the C_{31} alkane is greatly reduced in *cer3* mutants and even in the *far* mutants that are merely deficient in primary alcohols. The *far* mutants do not exhibit an elevated rate of cuticular water loss. More strikingly, their recovery following drought is greatly improved, indicating that fatty alcohols are unessential for drought response. This leads to the question of what is the disadvantage in losing primary alcohols specifically and exhibiting a glossy appearance in general. Since the glossy phenotype is dependent on optical parameters, we examined photosynthetic efficiency as well as light response. In both cases, there was no correlation between leaf glossiness and these parameters. In *Eucalyptus* species, it was shown that glaucous leaves had the effect of reducing photosynthesis before saturating conditions. In addition, in these plants, once the wax was removed, photoinhibition occurred at a high light intensity, while this did not occur in untreated plants (Cameron, 1970). We initially hypothesized that similar to the findings of Cameron (1970), the glossy mutants would reach photoinhibition at a lower light intensity and have higher carbon assimilation at a nonsaturating light intensity. However, this was not the case in the four mutants examined in this study, and the *cer1* mutant line even assimilated carbon at lower rates with rising light intensity.

Epicuticular wax has been suggested to play a protective role against a range of stresses. Drought (Aharoni *et al.*, 2004; Seo *et al.*, 2011; Lee *et al.*, 2014; Lee & Suh, 2015; Xue *et al.*, 2017), UV radiation (Long *et al.*, 2003), osmotic stress (Liu *et al.*, 2019), and insect herbivory (reviewed in Eigenbrode & Espelie, 1995) are a few such conditions. However, under our experimental conditions, we did not find a common disadvantage in coping with abiotic stress conditions, which is linked to a glossy appearance. Hence, a glaucous appearance may have a positive effect when combating abiotic stress conditions that were not tested in this study.

Conclusions

The examination of epicuticular wax mutants in *N. glauca* revealed that while alkane accumulation is strongly correlated with decreased cuticular water loss, under well-watered conditions, the epicuticular wax composition does not affect whole-plant *N. glauca* water loss or growth rate. Despite this, alkanes greatly affected the ability of plants to recover following drought conditions, since they sealed the cuticle and prevented water loss when stomata were closed, preventing leaf death. Furthermore, alkane deficiency led to a previously unobserved phenotype of stem cracking. Under our experimental conditions, we could not find a common denominator between plants possessing a glossy phenotype. By contrast, only plants in which cutin was strongly affected displayed an altered photosynthetic efficiency and light response, emphasizing the importance of uncoupling cutin-related effects from those that are epicuticular wax derived.

Acknowledgements

We thank Prof. Björn Usadel for providing us with access to unpublished *N. glauca* genomic and transcriptomics data. The work in the AA laboratory was supported by the Israel Science Foundation personal grant (no. 2089/18). We thank the Adelis Foundation, Leona M. and Harry B. Helmsley Charitable Trust, Jeanne and Joseph Nissim Foundation for Life Sciences, Tom and Sondra Rykoff Family Foundation Research, and the Raymond Burton Plant Genome Research Fund for supporting the AA lab activity. AA is the incumbent of the Peter J. Cohn Professorial Chair. Support for this work was also provided by Weizmann Institute's Sustainability and Energy Research Initiative (SAERI) fellowship and USDA postdoctoral fellowship no. 2022-67012-36739.

Competing interests

None declared.

Author contributions

BN designed and performed experiments, analyzed the data, and wrote the manuscript. SH-A performed experiments. EA-S performed transcriptomic assembly and analysis. LS performed and analyzed experiments. GJ supervised gum arabic wax extraction and profiling. AA planned and supervised the study and edited the manuscript.

ORCID

Asaph Aharoni https://orcid.org/0000-0002-6077-1590
Shelly Hen-Avivi https://orcid.org/0000-0002-9949-3743
Georg Jander https://orcid.org/0000-0002-9675-934X
Boaz Negin https://orcid.org/0000-0003-1890-9848

Data availability

The data that support the findings of this study are openly available in NCBI SRA repository at https://www.ncbi.nlm.nih.gov/bioproject/PRJNA765497/, no. PRJNA765497.

References

Aarts MG, Keijzer CJ, Stiekema WJ, Pereira A. 1995. Molecular characterization of the *CER1* gene of Arabidopsis involved in epicuticular wax biosynthesis and pollen fertility. *Plant Cell* **11**: 825–838.

Adato A, Mandel T, Mintz-Oron S, Venger I, Levy D, Yativ M, Domínguez E, Wang Z, De Vos RCH, Jetter R *et al.* 2009. Fruit-surface flavonoid accumulation in tomato is controlled by a SLMYB12-regulated transcriptional network. *PLoS Genetics* **5**: e1000777.

Aharoni A, Dixit S, Jetter R, Thoenes E, van Arkel G, Pereira A. 2004. The SHINE clade of AP2 domain transcription factors activates wax biosynthesis, alters cuticle properties, and confers drought tolerance when overexpressed in Arabidopsis. *Plant Cell* **16**: 2463–2480.

Alcerito T, Barbo FE, Negri G, Santos DYAC, Meda CI, Young MCM, Chávez D, Blatt CTT. 2002. Foliar epicuticular wax of *Arrabidaea brachypoda*: flavonoids and antifungal activity. *Biochemical Systematics and Ecology* **30**: 677–683.

Bach L, Michaelson LV, Haslam R, Bellec Y, Gissot L, Marion J, Da Costa M, Boutin J-P, Miquel M, Tellier F *et al.* 2008. The very-long-chain hydroxy fatty acyl-CoA dehydratase PASTICCINO2 is essential and limiting for plant development. *Proceedings of the National Academy of Sciences, USA* **105**: 14727–14731.

Barthlott W, Neinhuis C, Cutler D, Ditsch F, Meusel I, Theisen I, Wilhelmi H. 1998. Classification and terminology of plant epicuticular waxes. *Botanical Journal of the Linnean Society* **126**: 237–260.

Beaudoin F, Wu X, Li F, Haslam RP, Markham JE, Zheng H, Napier JA, Kunst L. 2009. Functional characterization of the Arabidopsis β-ketoacyl-coenzyme a reductase candidates of the fatty acid elongase. *Plant Physiology* **150**: 1174–1191.

Bickford CP. 2016. Ecophysiology of leaf trichomes. *Functional Plant Biology* **43**: 807–814.

Bourdenx B, Bernard A, Domergue F, Pascal S, Leger A, Roby D, Pervent M, Vile D, Haslam RP, Napier JA *et al.* 2011. Overexpression of Arabidopsis *ECERIFERUM1* promotes wax very-long-chain alkane biosynthesis and influences plant response to biotic and abiotic stresses. *Plant Physiology* **156**: 29–45.

Cameron AD. 2019. Mitigating the risk of drought-induced stem cracks in conifers in a changing climate. *Scandinavian Journal of Forest Research* **34**: 667–672.

Cameron KD, Teece MA, Smart LB. 2006. Increased accumulation of cuticular wax and expression of lipid transfer protein in response to periodic drying events in leaves of tree tobacco. *Plant Physiology* **140**: 176–183.

Cameron RJ. 1970. Light intensity and the growth of *Eucalyptus* seedlings. The effect of cuticular waxes on light absorption in leaves of *Eucalyptus* species. *Australian Journal of Botany* **18**: 275–284.

Chalker-Scott L. 1999. Environmental significance of anthocyanins in plant stress responses. *Photochemistry and Photobiology* **70**: 1–9.

Chen X, Goodwin SM, Boroff VL, Liu X, Jenks MA. 2003. Cloning and characterization of the *WAX2* gene of Arabidopsis involved in cuticle membrane and wax production. *Plant Cell* **15**: 1170–1185.

Cohen H, Dong Y, Szymanski J, Lashbrooke J, Meir S, Almekias-Siegl E, Zeisler-Diehl VV, Schreiber L, Aharoni A. 2019. A multilevel study of melon fruit reticulation provides insight into skin ligno-suberization hallmarks. *Plant Physiology* **179**: 1486–1501.

Dalal A, Shenhar I, Bourstein R, Mayo A, Grunwald Y, Averbuch N, Attia Z, Wallach R, Moshelion M. 2020. A telemetric, gravimetric platform for real-time physiological phenotyping of plant–environment interactions. *Journal of Visualized Experiments* **2020**: 1–28.

Eigenbrode SD, Espelie KE. 1995. Effects of plant epicuticular lipids on insect herbivores. *Annual Review of Entomology* **40**: 171–194.

Greer S, Wen M, Bird D, Wu X, Samuels L, Kunst L, Jetter R. 2007. The cytochrome P450 enzyme CYP96A15 is the midchain alkane hydroxylase responsible for formation of secondary alcohols and ketones in stem cuticular wax of Arabidopsis. *Plant Physiology* **145**: 653–667.

Haas BJ, Papanicolaou A, Yassour M, Grabherr M, Blood PD, Bowden J, Couger MB, Eccles D, Li B, Lieber M *et al.* 2013. *De novo* transcript sequence reconstruction from RNA-seq using the Trinity platform for reference generation and analysis. *Nature Protocols* **8**: 1494–1512.

Halperin O, Gebremedhin A, Wallach R, Moshelion M. 2017. High-throughput physiological phenotyping and screening system for the characterization of plant–environment interactions. *The Plant Journal* **89**: 839–850.

Hanley ME, Lamont BB, Fairbanks MM, Rafferty CM. 2007. Plant structural traits and their role in anti-herbivore defence. *Perspectives in Plant Ecology, Evolution and Systematics* **8**: 157–178.

Hen-Avivi S, Savin O, Racovita RC, Lee W-S, Adamski NM, Malitsky S, Almekias-Siegl E, Levy M, Vautrin S, Bergès H *et al.* 2016. A metabolic gene cluster in the wheat W1 and the barley Cer-cqu loci determines b-diketone biosynthesis and glaucousness. *Plant Cell* **28**: 1440–1460.

Jetter R, Riederer M. 2016. Localization of the transpiration barrier in the epi- and intracuticular waxes of eight plant species: water transport resistances are associated with fatty acyl rather than alicyclic components. *Plant Physiology* **170**: 921–934.

Lange H, Ndecky SYA, Gomez-Diaz C, Pflieger D, Butel N, Zumsteg J, Kuhn L, Piermaria C, Chicher J, Christie M *et al.* 2019. RST1 and RIPR connect the cytosolic RNA exosome to the Ski complex in Arabidopsis. *Nature Communications* **10**: 3871.

Lee SB, Kim H, Kim RJ, Suh MC. 2014. Overexpression of Arabidopsis *MYB96* confers drought resistance in *Camelina sativa* via cuticular wax accumulation. *Plant Cell Reports* **33**: 1535–1546.

Lee SB, Suh MC. 2015. Advances in the understanding of cuticular waxes in *Arabidopsis thaliana* and crop species. *Plant Cell Reports* **34**: 557–572.

Leide J, Hildebrandt U, Reussing K, Riederer M, Vogg G. 2007. The developmental pattern of tomato fruit wax accumulation and its impact on cuticular transpiration barrier properties: effects of a deficiency in a β-ketoacyl-coenzyme A synthase (*LeCER6*). *Plant Physiology* **144**: 1667–1679.

Leide J, Hildebrandt U, Vogg G, Riederer M. 2011. The positional sterile (ps) mutation affects cuticular transpiration and wax biosynthesis of tomato fruits. *Journal of Plant Physiology* **168**: 871–877.

Li F, Wu X, Lam P, Bird D, Zheng H, Samuels L, Jetter R, Kunst L. 2008. Identification of the wax ester synthase/acyl-coenzyme A:diacylglycerol acyltransferase WSD1 required for stem wax ester biosynthesis in Arabidopsis. *Plant Physiology* **148**: 97–107.

Liu N, Chen J, Wang T, Li Q, Cui P, Jia C, Hong Y. 2019. Overexpression of *WAX INDUCER1/SHINE1* gene enhances wax accumulation under osmotic stress and oil synthesis in *Brassica napus*. *International Journal of Molecular Sciences* **20**: 4435.

Long LM, Prinal Patel H, Cory WC, Stapleton AE. 2003. The maize epicuticular wax layer provides UV protection. *Functional Plant Biology* **30**: 75–81.

Long N, Ren X, Xiang Z, Wan W, Dong Y. 2016. Sequencing and characterization of leaf transcriptomes of six diploid *Nicotiana* species. *Journal of Biological Research* **23**: 6.

Lü S, Song T, Kosma DK, Parsons EP, Rowland O, Jenks MA. 2009. Arabidopsis *CER8* encodes LONG-CHAIN ACYL-COA SYNTHETASE 1 (LACS1) that has overlapping functions with LACS2 in plant wax and cutin synthesis. *The Plant Journal* **59**: 553–564.

Millar AA, Clemens S, Zachgo S, Giblin EM, Taylor DC, Kunst L, Michael Giblin E, Taylor DC, Kunst L. 1999. *CUT1*, an Arabidopsis gene required for cuticular wax biosynthesis and pollen fertility, encodes a very-long-chain fatty acid condensing enzyme. *Plant Cell* **11**: 825–838.

Millar AA, Kunst L. 1997. Very-long-chain fatty acid biosynthesis is controlled through the expression and specificity of the condensing enzyme. *The Plant Journal* **12**: 121–131.

Mintz-Oron S, Mandel T, Rogachev I, Feldberg L, Lotan O, Yativ M, Wang Z, Jetter R, Venger I, Adato A *et al.* 2008. Gene expression and metabolism in tomato fruit surface tissues. *Plant Physiology* **147**: 823–851.

Mortimer CL, Bramley PM, Fraser PD. 2012. The identification and rapid extraction of hydrocarbons from *Nicotiana glauca*: a potential advanced renewable biofuel source. *Phytochemistry Letters* **5**: 455–458.

Negin B, Moshelion M. 2017. The advantages of functional phenotyping in pre-field screening for drought-tolerant crops. *Functional Plant Biology* **44**: 107–118.

Pascal S, Bernard A, Deslous P, Gronnier J, Fournier-Goss A, Domergue F, Rowland O, Joubès J. 2019. Arabidopsis CER1-LIKE1 functions in a cuticular very-long-chain alkane-forming complex. *Plant Physiology* **179**: 415–432.

Peiffer M, Tooker JF, Luthe DS, Felton GW. 2009. Plants on early alert: glandular trichomes as sensors for insect herbivores. *New Phytologist* **184**: 644–656.

Richards R, Rawson H, Johnson D. 1986. Glaucousness in wheat: its development and effect on water-use efficiency, gas exchange and photosynthetic tissue temperatures. *Functional Plant Biology* **13**: 465.

Roth-Nebelsick A, Fernández V, Peguero-Pina JJ, Sancho-Knapik D, Gil-Pelegrín E. 2013. Stomatal encryption by epicuticular waxes as a plastic trait modifying gas exchange in a Mediterranean evergreen species (*Quercus coccifera* L.). *Plant, Cell & Environment* **36**: 579–589.

Rowland O, Zheng H, Hepworth SR, Lam P, Jetter R, Kunst L. 2006. *CER4* encodes an alcohol-forming fatty acyl-coenzyme A reductase involved in cuticular wax production in Arabidopsis. *Plant Physiology* **142**: 866–877.

Ryan KG, Swinny EE, Markham KR, Winefield C. 2002. Flavonoid gene expression and UV photoprotection in transgenic and mutant *Petunia* leaves. *Phytochemistry* **59**: 23–32.

Ryan KG, Swinny EE, Winefield C, Markham KR. 2001. Flavonoids and UV photoprotection in Arabidopsis mutants. *Zeitschrift fur Naturforschung – Section C Journal of Biosciences* **56**: 745–754.

Sarrion-Perdigones A, Vazquez-Vilar M, Palací J, Castelijns B, Forment J, Ziarsolo P, Blanca J, Granell A, Orzaez D. 2013. Goldenbraid 2.0: a comprehensive DNA assembly framework for plant synthetic biology. *Plant Physiology* **162**: 1618–1631.

Schnurr J, Shockey J, Browse J. 2004. The acyl-CoA synthetase encoded by *LACS2* is essential for normal cuticle development in Arabidopsis. *Plant Cell* **16**: 629–642.

Seo PJ, Lee SB, Suh MC, Park MJ, Park CM. 2011. The MYB96 transcription factor regulates cuticular wax biosynthesis under drought conditions in Arabidopsis. *Plant Cell* **23**: 1138–1152.

Simpson JP, Ohlrogge JB. 2016. A novel pathway for triacylglycerol biosynthesis is responsible for the accumulation of massive quantities of glycerolipids in the surface wax of bayberry (*Myrica pensylvanica*) fruit. *Plant Cell* **28**: 248–264.

Sonawane PD, Jozwiak A, Panda S, Aharoni A. 2020. 'Hijacking' core metabolism: a new panache for the evolution of steroidal glycoalkaloids structural diversity. *Current Opinion in Plant Biology* **55**: 118–128.

Steffens JC, Walters DS. 1991. Biochemical aspects of glandular trichome-mediated insect resistance in the Solanaceae. *ACS Symposium Series* **449**: 136–149.

Usadel B, Tohge T, Scossa F, Sierro N, Schmidt M, Vogel A, Bolger A, Kozlo A, Enfissi EM, Morrel K *et al.* 2018. The genome and metabolome of the tobacco tree, *Nicotiana glauca*: a potential renewable feedstock for the bioeconomy. *bioRxiv*. doi: 10.1101/351429.

Xue D, Zhang X, Lu X, Chen G, Chen ZH. 2017. Molecular and evolutionary mechanisms of cuticular wax for plant drought tolerance. *Frontiers in Plant Science* **8**: 621.

Yaaran A, Negin B, Moshelion M. 2019. Role of guard-cell ABA in determining maximal stomatal aperture and prompt vapor-pressure-deficit response. *Plant Science* **281**: 31–40.

Yeats TH, Rose JKC. 2013. The formation and function of plant cuticles. *Plant Physiology* **163**: 5–20.

Zeisler V, Schreiber L. 2016. Epicuticular wax on cherry laurel (*Prunus laurocerasus*) leaves does not constitute the cuticular transpiration barrier. *Planta* **243**: 65–81.

Zeisler-Diehl V, Müller Y, Schreiber L. 2018. Epicuticular wax on leaf cuticles does not establish the transpiration barrier, which is essentially formed by intracuticular wax. *Journal of Plant Physiology* **227**: 66–74.

Zeltiņš P, Katrevičs J, Gailis A, Maaten T, Baders E, Jansons A. 2018. Effect of stem diameter, genetics, and wood properties on stem cracking in Norway spruce. *Forests* **9**: 546.

Zheng H, Rowland O, Kunst L. 2005. Disruptions of the Arabidopsis enoyl-CoA reductase gene reveal an essential role for very-long-chain fatty acid synthesis in cell expansion during plant morphogenesis. *Plant Cell* **17**: 1467–1481.

Supporting Information

Additional Supporting Information may be found online in the Supporting Information section at the end of the article.

Fig. S1 Gene structure and crRNA locations on nine of the genes targeted for genome editing.

Fig. S2 Transcriptional profiles of 16 *Nicotiana glauca* genes in five tissues under well-watered and drought conditions.

Fig. S3 Additional genome-edited plants phenotypes.

Fig. S4 Abundance of 11 additional epicuticular wax components in wild-type and mutant plants.

Fig. S5 Abundance of the six major wax components extracted using the gum arabic method.

Fig. S6 Abundance of 17 additional epicuticular wax components extracted using gum arabic.

Fig. S7 Ratio of the main wax components extracted using chloroform or gum arabic.

Fig. S8 Relative abundance of cutin and its monomers in mutant lines.

Fig. S9 Correlation of cuticular water loss rate to total wax load.

Fig. S10 *cer3* mutants' response to full irrigation, drought, and recovery (summer experiment).

Fig. S11 *cer3* mutants' response to full irrigation, drought, and recovery (winter experiment).

Fig. S12 Images of mutant plants at the end of the spring drought experiment.

Fig. S13 Stem cracking phenomenon.

Fig. S14 Effects of wax composition on stomatal size, density, and aperture.

Fig. S15 Negative correlation of stomatal density and size.

Fig. S16 Transcriptomic profiles of *Nicotiana glauca CER3* and *CER1* homologs.

Methods S1 Full descriptions of experimental methods used in this study, and not fully described in the main text.

Table S1 Chloroform extracted wax components in individual wild-type and wax mutant plants.

Table S2 Extracted cutin components in individual wild-type and wax mutant plants.

Please note: Wiley is not responsible for the content or functionality of any Supporting Information supplied by the authors. Any queries (other than missing material) should be directed to the *New Phytologist* Central Office.